Buddleja saligna Willd (Loganiaceae) inhibits angiotensin-converting enzyme activity in oxidative cardiopathy with concomitant modulation of nucleotide hydrolyzing enzymatic activities and dysregulated lipid metabolic pathways

Ochuko L. Erukainure[a], Chika I. Chukwuma[b], Motlalepula G. Matsabisa[a,*], Veronica F. Salau[c], Neil A. Koorbanally[d], Md Shahidul Islam[c]

[a] *Department of Pharmacology, School of Clinical Medicine, Faculty of Health Sciences, University of the Free State, Bloemfontein, 9300, South Africa*
[b] *Department of Health Sciences, Faculty of Health and Environmental Sciences, Central University of Technology, Bloemfontein, 9300, South Africa*
[c] *Department of Biochemistry, School of Life Sciences, University of KwaZulu-Natal, (Westville Campus), Durban, 4000, South Africa*
[d] *School of Chemistry and Physics, University of KwaZulu-Natal, (Westville Campus), Durban, 4000, South Africa*

ARTICLE INFO

ABSTRACT

Ethnopharmacological relevance: *Buddleja saligna* Willd (Loganiaceae), mostly indigenous to South Africa is traditionally used in the treatment cardio-dysfunctional related ailments amongst other diseases.
Aims: The cardio-protective effect of *B. saligna* was investigated in ferric-induced oxidative cardiopathy.
Methods: Hearts harvested from healthy male SD rats were incubated with 0.1 mM FeSO$_4$ to induce oxidative damage and co-incubated with *B. saligna* extract. Reaction mixtures without the extract served as negative control, while tissues without the extract or standard antioxidant (gallic acid) and pro-oxidant served as the normal control. The tissues were analyzed for levels of glutathione, malondialdehyde, and nitric oxide as well as cholinergic, angiotensin-converting enzyme (ACE), lipase, and purinergic enzymes activities, lipid profiles, fatty acid metabolic pathways and metabolites.
Results: Induction of oxidative damage significantly ($p < 0.05$) depleted the levels of GSH, SOD, catalase, and ENTPDase activities, while concomitantly elevating the levels of MDA, NO, ACE, acetylcholinesterase, lipase and ATPase activities. These levels and activities were significantly reversed on treatment with *B. saligna*. Treatment with *B. saligna* also led to depletion of cardiac cholesterol and LDL-c levels, while elevating triglyceride and HDL-c level. It also depleted oxidative-induced lipid metabolites with concomitant generation of thirteen other metabolites. *B. saligna* also inactivated oxidative-induced pathways for beta oxidation of very long chain fatty acids, glycerolipid metabolism, and fatty acid elongation in mitochondria.
Conclusion: These results suggest that *B. saligna* protects against ferric-induced oxidative cardiopathy by mitigating oxidative stress, while concomitantly inhibiting ACE, acetylcholinesterase and lipase activities, and modulating lipid spectrum and dysregulated metabolic pathways.

1. Introduction

Cardiopathy has been recognized as one of the leading contributors of early mortality in both developed and developing countries (Poulter, 2003; Wold et al., 2005). Hyperlipidemia (characterized by elevated LDL-c and depleted HDL-c levels), hypertension, smoking, diabetes, and obesity have been reported as some of the most modifiable risks factors of cardiopathy (Poulter, 2003). Disorder in cardiac energy metabolism including defects of lipid metabolism (particularly the β-oxidation pathway) and mitochondrial oxidative phosphorylation are amongst the common mechanism of cardiopathy (Antozzi and Zeviani, 1997).

These defects often lead to the accumulation of leaked reactive oxygen species (ROS), which when supersedes the body's endogenous antioxidant defense system will lead to oxidative stress. Oxidative stress has been implicated in the pathogenesis and progress of cardiopathy and other cardiovascular dysfunctions (Antozzi and Zeviani, 1997; Gammella et al., 2015; Wold et al., 2005). This is evidenced in the therapeutic target of oxidative stress in the treatment and management of cardiovascular diseases (De Blasio et al., 2015; Huynh et al., 2013, 2014). Studies have also linked oxidative stress with the exacerbation of markers associated with cardiopathy such as increased activities of angiotensin-converting enzyme (ACE) and acetylcholinesterase

(Kovacic and Thurn, 2005; Shirpoor et al., 2009; Wojciechowska et al., 2014).

The use of medicinal plants in the management and treatment of cardiovascular disease (CVD) and other diseases has been well documented (Chukwuma et al., 2019; Jaradat, 2005; Mashour et al., 1998). This has been attributed to their phytochemical and nutritional constituents (Chukwuma et al., 2019). Some of these plants have over the years been developed into nutraceuticals and used as adjunct therapy. Amongst such plants is *Buddleja saligna* Willd.

Buddleja saligna Willd (South African Tree No. 636) is an evergreen tree of medium size widely distributed in South Africa, where it is grows on rocky hillsides and/or along watercourses (Adedapo et al., 2009). Its common English names are false and/or bastard olive. It is also known as *umceba* and *igqeba-elimhlophe* in Zulu, *umBatacwepe* in Siswati, *mothlware* in Tswana, *witolien* in Afrikaans, *unGqeba* in Xhosa, and *lelothwane* in Sotho (Aubrey, 2002; Chukwujekwu et al., 2014). In folkloric medicine, it is used in the treatment of high blood pressures, chest pains, coughs, diabetes, colds, tuberculosis, and anasarca (Adedapo et al., 2009; Chukwujekwu et al., 2014). Its anti-inflammatory, anti-malaria, antioxidant, and antibacterial activities have also been reported (Adedapo et al., 2009; Chukwujekwu et al., 2014, 2016).

Despite its folkloric uses, there is still a dearth in the scientific efficacy on the use of *B. saligna* in the treatment and management of cardiovascular related ailments. Thus, the aim of this study was to investigate the cardio-protective effect of *B. saligna* by determining its ability to stall redox imbalance, activities of angiotensin-converting enzyme (ACE) activity, and modulate cholinergic and purinergic activities, and lipid metabolism in oxidative cardiopathy.

2. Materials and methods

2.1. Plant material and extraction

Fresh stocks of *B. saligna* were collected from Free State Province, South Africa (GPS coordinates: 32°43′25.5″S 26°53′28.2″E & 32°43′51.0″S 26°53′29.0″E). Plant sample was deposited by Matsabisa M.G. and authenticated at the Geo Potts herbarium (BLFU), University of the Free State (specimen voucher number: BLFU/MGM0015). The plant's name was also checked with http://www.theplantlist.org (http://www.theplantlist.org/tpl1.1/record/kew-2685596).

The plant sample was washed and air-dried roots were pulverized into fine powder. The powdered sample (100 g in a 1:5 mass:solvent ratio in mL) was extracted using hexane, dichloromethane (DCM), methanol & dichloromethane (MeOH:DCM; 1:1, v/v) and methanol (MeOH) sequentially. Extraction was done for 24 h, at ambient room temperature with mild agitation of 100 rpm. After extraction, each solvent was filtered and concentrated using an R – 215 rotary evaporator (Buchi, Switzerland). Concentrated extracts were air-dried and stored at 4 °C.

2.2. Enzyme inhibitory activity

2.2.1. ACE activity

The resulting extracts were screened for their anti-hypertensive potentials by determining their inhibitory effect on ACE activity *in vitro* (Shalaby et al., 2006). Briefly, 10 μL of ACE solution (250 mU/mL) and 10 μL of different concentrations of plant extract or positive control (captopril) or assay buffer (50 mM Tris-HCl with 300 mM NaCl, pH 7.5) (control) was mixed in a 96 well plate and incubated on ice for 10 min. Thereafter, 150 μL pre-warmed (37 °C) substrate solution (1.75 mM of FAPGG in assay buffer) was be added and mixed. The final concentrations of extract and captopril in the reaction mixture were 15–120 μg/mL and 0.001–100 μM, respectively. Absorbance was immediately measured at 340 nm and monitored at 37 °C for 15 min at 1 min interval (Multiskan™ GO Microplate Spectrophotometer, Thermo

Scientific™, Massachusetts, United States). A linear graph of absorbance vs time (min) was plotted and the slope of graph will be calculated. ACE activity inhibition was calculated using the following formula:

$$Inhibition(\%) = \frac{(Slope\ of\ control - Slope\ of\ test)}{Slope\ of\ control} x100$$

2.2.2. Renin activity

Based on the results which results, the anti-hypertensive potential of MeOH:DCM extract was further evaluated by investigating its inhibitory effect on renin activity. Renin was measured using the an Abcam ab204723 Renin Inhibitor Screening Assay Kit (Fluorometric) (cambridge, UK) according to the kit's described protocol. The extract was tested at concentrations of 25, 50 and 100 μg/mL, while a standard renin inhibitor (aliskerin) was used as a positive control at concentrations of 12.5 nM–200 nM. Fluorescence was measured using a Synergy™ HT Multi-Mode Microplate Reader (BioTek Instruments, Inc., Winooski, United States).

The MEOH:DCM fraction was chosen for further *ex vivo* study.

2.3. Animals

Four male albino rats (Sprague Dawley strain) weighing 200–250 g were obtained from the Biomedical Research Unit (BRU), University of KwaZulu-Natal, Durban, South Africa. The rats were fasted overnight (12 h) before euthanizing with isofor. Their hearts were collected and rinsed in 0.9% NaCl solution to remove blood stains. They were homogenized in 50 mM sodium phosphate buffer (pH 7.5; with 1% Triton X-100), and thereafter centrifuged at 15,000 rpm at 4 °C for 10 min. The supernatants (lysates) were collected for *ex vivo* studies.

The study was conducted under the approved guidelines of the Animal Ethics Committee of the University of KwaZulu-Natal, Durban, South Africa (Protocol approval number: AREC/020/017D).

2.4. Induction of oxidative injury ex vivo

An aliquot of 100 μL of the cardiac tissue lysate was incubated with an equal volume of different concentrations (30, 60, 120 and 240 μg/mL) of the MEOH:DCM extract of *B. saligna* and 30 μL of pro-oxidant (0.1 mM FeSO₄) at 37 °C for 30 min (Erukainure et al., 2017a, 2017b). Reaction mixture without the extract served as negative control (untreated), while tissue lysates without the extract and pro-oxidant served as the normal control. Gallic acid was used as the standard antioxidant drug.

2.5. Antioxidative activities

The antioxidant status of the tissue lysates was determined by analyzing the reduced glutathione (GSH) level (Ellman, 1959), catalase and superoxide dismutase (SOD) activities (Aebi, 1984; Kakkar et al., 1984) and malondialdehyde (MDA) level (Chowdhury and Soulsby, 2002).

2.5.1. Reduced glutathione (GSH) level

Briefly, the tissue lysates was deproteinized by mixing an equal volume of 10% TCA and then centrifuged for 5 min at 3500 rpm 200 μL of the supernatants was thereafter collected into a 96 well plate, to which 50 μL of Ellman reagent was added. The reaction mixture was incubated for 5 min before reading absorbance at 415 nm. The GSH level was of the tissues was extrapolated from a standard curve of plotted GSH concentrations.

2.5.2. Superoxide dismutase (SOD) activity

Briefly, 15 μL of the tissue lysates were mixed with 170 μL of 0.1 mM diethylenetriaminepentaacetic acid (DETAPAC) in a 96 well

plate. 15 μL of freshly prepared 1.6 mM 6-hydroxydopamine (6-HD) was thereafter added. Absorbance of the reactant mixture was measured at 492 nm for 5 min at 1 min interval.

2.5.3. Catalase activity

Briefly, 10 μL of the tissue lysates was added to 340 μL of 50 mM sodium phosphate buffer (pH 7.0). 150 μL of 2M hydrogen peroxide (H_2O_2) was then added to the reaction mixture. Absorbance was read at 240 nm at 1 min interval for 3 min.

2.5.4. Lipid peroxidation levels

Briefly, 100 μL of the tissue lysates was mixed with 100 μL of 8.1% SDS solution, 375 μL of 20% acetic acid, and 1 mL of 0.25% thiobarbituric acid (TBA). The reaction mixture was boiled at 95 °C for 1 h in a water bath. 200 μL of the reaction mixture was thereafter pipetted into 96-well plate, and absorbance read at 532 nm.

2.6. Nitric oxide level

The Griess method was employed in the determining the nitric oxide (NO) level of the tissue lysates as previously described (Erukainure et al., 2019; Tsikas, 2005). Briefly, 100 μL of the tissue lysates was mixed with an equal volume of Griess reagent and incubated at 25 °C for 30 min in the dark. Distilled water served as the blank. Absorbance was read at 548 nm.

2.7. ACE activity

The ACE activity of the tissue lysates was determined spectrophotometrically using N-[3-(2-Furyl) acryloyl]-L-phenylalanyl-glycyl-glycine (FAPGG) as substrate (Holmquist et al., 1979) with slight modifications. Briefly, 20 μL of the reaction samples were incubated with 100 μL of 0.5 mM FAPGG for 10 min at 37 °C. Absorbance was read at 345 nm at 2 min intervals. The activity was expressed as the rate of reaction (ΔA/min) as calculated below:

$$ACE\ activity = \frac{(AI - AF)Sample - (AI - AF)Blank}{Time\ interval\ (min)}$$

Where AI = initial absorbance; AF = final absorbance.

2.8. Cholinergic enzymes activities

The cholinergic status of the tissue lysates was determined by analyzing the acetylcholinesterase activity using the Ellman's procedure (Ellman et al., 1961). Briefly, 20 μL of the tissue lysates was incubated with 10 μL of 3.3 mM Ellman's reagent (pH 7.0) and 50 μL of 0.1 M phosphate buffer (pH 8) for 20 min at 25 °C 10 μL of 0.05 M acetylcholine iodide was thereafter added to the reaction mixture. Absorbance was read at 412 nm at 3 min intervals.

2.9. Purinergic enzymes activities

The purinergic enzyme activities of the tissue lysates were determined by analyzing the activities of adenylpyrophosphatase (ATPase) (Adewoye et al., 2000; Erukainure et al., 2017a) and ecto-nucleoside triphosphate diphosphohydrolase (ENTPDase) (Akomolafe et al., 2017) respectively.

2.9.1. Determination of ATPase activity

Briefly, 200 μL of the tissue lysates was mixed with 200 μL of 5 mM KCl, 1300 μL of 0.1 M Tris-HCl buffer, and 40 μL of 50 mM ATP. The reaction mixture was then incubated at 37 °C in a shaker for 30 min. After incubation, 1 mL of distilled water and 1.25% ammonium molybdate were added to the reaction mixture. 1 mL of freshly prepared 9% ascorbic acid was thereafter added to the reaction mixture and allowed to stand for 30 min. Absorbance was read at 660 nm.

2.9.2. Determination of E-NTPDase activity

Briefly, 20 μL of the tissue lysates was mixed with 200 μL of the reaction buffer (1.5 mM $CaCl_2$, 5 mM KCl, 0.1 mM EDTA, 10 mM glucose, 225 mM sucrose and 45 mM Tris-HCl) and incubated at 37 °C for 10 min. Thereafter, 20 μL of 50 mM ATP was added to the reaction mixture and further incubated in a shaker for 20 min at 37 °C. The reaction was stopped by adding 200 μL of 10% TCA to the reaction mixture. The reaction was incubated in ice for 10 min and absorbance was read 600 nm.

2.10. Lipase activity

The lipase activity was determined using a previous described protocol (Kim et al., 2010) with slight modification. Briefly, 100 μL of the tissue lysates were incubated with 169 μL of Tris buffer (100 mM Tris–HC1 and 5 mM $CaCl_2$, pH 7.0) at 37 °C for 15 min. Thereafter, 5 μL of 10 mM p-NPB (p-nitrophenyl butyrate in dimethyl formamide) was added to the reaction mixture and further incubated at 37 °C for 15 min. Absorbance was read at 405 nm at 1 min interval. Lipase activity was expressed as the rate of reaction (ΔA/min).

2.11. Cardiac lipid profile

The cardiac tissues were incubated overnight with 0.1 mM $FeSO_4$ and 240 μg/mL of the plant extract or gallic acid as previously described in section 2.4 but overnight (12 h). The samples were centrifuged at 15,000 rpm for 10 min at 4 °C. The supernatants were collected and immediately assayed for lipid profile levels (total cholesterol, triglycerides, and HDL-cholesterol) using an Automated Chemistry Analyzer (Labmax Plenno, Labtest Co. Ltd., Lagoa Santa, Brazil) with commercial assay kits according to manufacturer's manual.

2.12. Metabolite extraction and profiling

The reaction mixture was prepared as described above. After incubation, lipid metabolites were extracted from the samples and subjected to gas chromatography-mass spectrometry (GC-MS) metabolic profiling with slight modification (Ralston-Hooper et al., 2011). Briefly, cold chloroform was added to the incubated samples at a ratio of 5:1 and vortexed for 1 min. The mixture was allowed to stand on ice for 20 min and thereafter centrifuged at 15,000 rpm at 4 °C for 10 min to yield 2 liquid phases. The lower phase (chloroform) layer containing the lipid metabolites and other non-polar metabolites was collected and profiled with GC-MS.

2.13. GC-MS analysis of lipid metabolites

The chloroform phase containing lipid and other non-polar metabolites were analyzed with GC-MS (Agilent technologies 6890 series GC coupled with (an Agilent) 5973 Mass Selective Detector and driven by Agilent Chemstation software). The operating parameters were as follows: **Column**: HP-5MS capillary column (30 m × 0.25 mm ID, 0.25 μm film thickness, 5% phenylmethylsiloxane); **Carrier gas**: ultra-pure helium; **Flow rate**: 1.0 mL/min and a linear velocity of 37 cm s⁻¹; **Injector temperature**: set at 250 °C. Initial oven temperature: 60 °C, programmed to 280 °C at the rate of 10 °C min⁻¹. **Injection**: 1 μL made in split mode at a split ratio of 20:1; **Electron ionization mode**: 70 eV; **Electron multiplier voltage**: at 1859 V; **Ion source temperature**: 230 °C; **Quadrupole temperature**: 150 °C; **Solvent delay**: 4 min; **Scan range**: 50–70 amu. Lipid metabolites were identified using an inbuilt NIST library.

2.14. Metabolic pathway analysis

In order to identify the most relevant pathways involved in lipid metabolism in the protective effect of *B. saligna* on oxidative

cardiopathy, the identified lipid metabolites were subjected to pathway enrichment analysis using the MetaboAnalyst 4.0 online server (Chong et al., 2018).

2.15. High-performance liquid chromatography (HPLC)

HPLC-diode array detection analysis of the MEOH:DCM extract was performed using an Agilent 1100 series (Agilent, Waldbronn, Germany) instrument equipped with photo diode array, autosampler, column thermostat and degasser. A Phenomenex: Luna 5 μm C_{18} (2) (150 × 4.6 mm; 5 μm particle size) column was used as the stationary phase. Water containing 0.01% of formic acid (A) and acetonitrile (B) served as mobile phases at a flow rate of 1 mL/min. Gradient elution was applied as follows: Initial ratio 95% A: 5% B, keeping for 10 min, changed to 90% A: 10% B in 10 min, changed to 70% A: 30% B in 10 min, to 50% A: 50% B in 10 min, maintaining for 0.5 min and back to initial ratio in 0.5 min. Temperature was set to 30 °C. The injection volume was 20.0 μL and chromatograms were recorded at 254 nm.

2.16. Statistical analysis

One-way analysis of variance (ANOVA) was used in analyzing the data and presented as mean ± SD. Significant differences between means at $p < 0.05$ were obtained with the Tukey's HSD-multiple range post-hoc test. Statistical analyses were done using IBM Statistical Package for the Social Sciences (SPSS) for Windows, version 23.0 (IBM Corp., Armonk, NY, USA). The GC-MS identified metabolites were subjected to statistical analysis using the MetaboAnalyst 4.0 online server (Chong et al., 2018).

3. Results

As shown in Fig. S1, the MEOH:DCM and DCM extracts significantly ($p < 0.05$) inhibited ACE activity dose dependently. The low IC_{50} value of 118.48 μg/mL for MEOH:DCM (Table 1), depicts it as the most active extract.

Further investigation of the anti-hypertensive potentials of MEOH:DCM extract revealed a significant ($p < 0.05$) inhibitory effect on renin activity in dose-dependent manner, with an IC_{50} value of 280.18 μg/mL (Table 1).

Incubation of cardiac tissue lysates with $FeSO_4$ led to significant ($p < 0.05$) depletion in the levels of GSH, SOD and catalase activities, while elevating MDA level as depicted in Fig. 1A – 1D. These levels and/or activities were significantly ($p < 0.05$) reversed on treatment with the MEOH:DCM extract.

There was a significant ($p < 0.05$) increase in the NO level of cardiac tissue lysates incubated with $FeSO_4$ as shown in Fig. 2. Treatment with the MEOH:DCM extract significantly ($p < 0.05$) reduced it to levels indistinguishable from the control.

As depicted in Fig. 3, there was an elevation in ACE activity of cardiac tissue lysates incubated with $FeSO_4$. The activity was significantly ($p < 0.05$) reduced dose-dependently on post treatment with the MEOH:DCM extract to levels indistinguishable from the control and

Table 1
IC_{50} values of studied *in vitro* biological activities.

Extracts	ACE activity	Renin activity
	(μg/mL)	
Hexane	−96.13	
Methanol	258.94	
Dichloromethane	204.32	
Methanol-Dichloromethane	118.48	280.18
Aqueous	486.52	

Data = mean; n = 3.

standard drug.

Incubation of cardiac tissue lysate with $FeSO_4$ led to significant ($p < 0.05$) increase in acetylcholinesterase activity as depicted in Fig. 4. This was significantly ($p < 0.05$) reduced dose-dependently on treatment with the MEOH:DCM extract.

Incubation of cardiac tissue lysate with $FeSO_4$ significantly ($p < 0.05$) elevated ATPase activity, with concomitant depletion of ENTPDase activity shown in Fig. 5A and B. These activities were however reversed dose-dependently on treatment with the MEOH:DCM extract.

Incubation of cardiac tissue lysates with $FeSO_4$ led to significant increase in cardiac lipase activity as depicted in Fig. 6. There was a significant ($p < 0.05$) dose-dependent decrease in the activity on treatment with the MEOH:DCM extract.

As depicted in Fig. 7, there was a significant ($p < 0.05$) elevation in the cardiac cholesterol and LDL-c levels, with concomitant depleted levels of triglycerides and HDL-c on incubation of cardiac tissues lysates with $FeSO_4$. These levels were significantly ($p < 0.05$) reversed on treatment with the MEOH:DCM extract.

As shown in Table 2, GC-MS analysis of the lipid metabolites of cardiac tissue lysates revealed the presence of fatty alkanes, fatty alkenes, fatty acyls, fatty alcohols, fatty acids, fatty acid esters, glycerol, fatty amides, glycols, steroids, and non-lipids. Induction of oxidative injury with $FeSO_4$ led to complete depletion of 2,3,6-Trimethyldecane; pentadecanoic acid, ethyl ester; 1-O-(22-Hydroxydocosyl)-d-mannitol; and retinal in cardiac tissues, with concomitant generation of squalene, tetracosanoic acid, palmitic acid, 9-Octadecenoic acid, (E)-, arachidic acid, ethyl ester and glycerol 1-palmitate. It also led to significant ($p < 0.05$) increase in cardiac cholesterol and cis-9, cis-12-Octadeca-dienoic acid concentrations (Fig. 8). Treatment with MEOH:DCM extract led to the complete depletion of the oxidative-induced metabolites: squalene; tetracosanoic acid; palmitic acid; 9-Octadecenoic acid, (E)-; and glycerol 1-palmitate, while concomitantly restoring cardiac cholesterol level. It also led to the generation of tetrahydroionol; non-ahexacontanoic acid; 2-dodecenoic acid; allyl decanoate; l-(+)-Ascorbic acid 2,6-dihexadecanoate; oleyl amide; (11. alpha.)-11-Methoxypregn-4-ene-3,20-dione; 25-hydroxycholesterol, dimethyl ether; 2,2-dimethoxycholestane; R1-Barrigenol; 24,25-dihydroxyvitamin D; cimarin; and alpha-terpineol.

Clustering analysis of the identified cardiac lipid metabolites revealed distinctive changes for all the experimental tissues as depicted by the negative values and heat intensity (Fig. 9A). Principal Component Analysis (PCA) of the metabolites also revealed distinctive changes in the treated tissues from the untreated as portrayed by the pairwise score plots between the selected PCs (Fig. 9B).

Pathway analysis of the identified lipid metabolites revealed deactivation of cardiac retinol metabolism pathway, with concomitant activation of pathways for bile acid biosynthesis, arachidonic acid metabolism, beta oxidation of very long chain fatty acids, glycerolipid metabolism, fatty acid elongation in mitochondria, fatty acid biosynthesis and fatty acid metabolism on induction of oxidative injury (Fig. 10). Treatment with the MEOH:DCM extract led to inactivation of the oxidative-induced pathways for beta oxidation of very long chain fatty acids, glycerolipid metabolism, and fatty acid elongation in mitochondria. It also inactivated bile acid biosynthesis and arachidonic acid metabolism pathways. These pathways are schematically presented in Fig. 11.

HPLC analysis of the MEOH:DCM extract revealed the presence of the phenolics: methyl gallate, ferulic acid and quercetin, with the least abundance being methyl gallate as depicted in Table 3.

4. Discussion

Cardiopathies such as cardiomyopathy arising from defects of energy metabolism rather than inherited cardiovascular dysfunction has been recognized amongst the major causes of global mortality (Antozzi
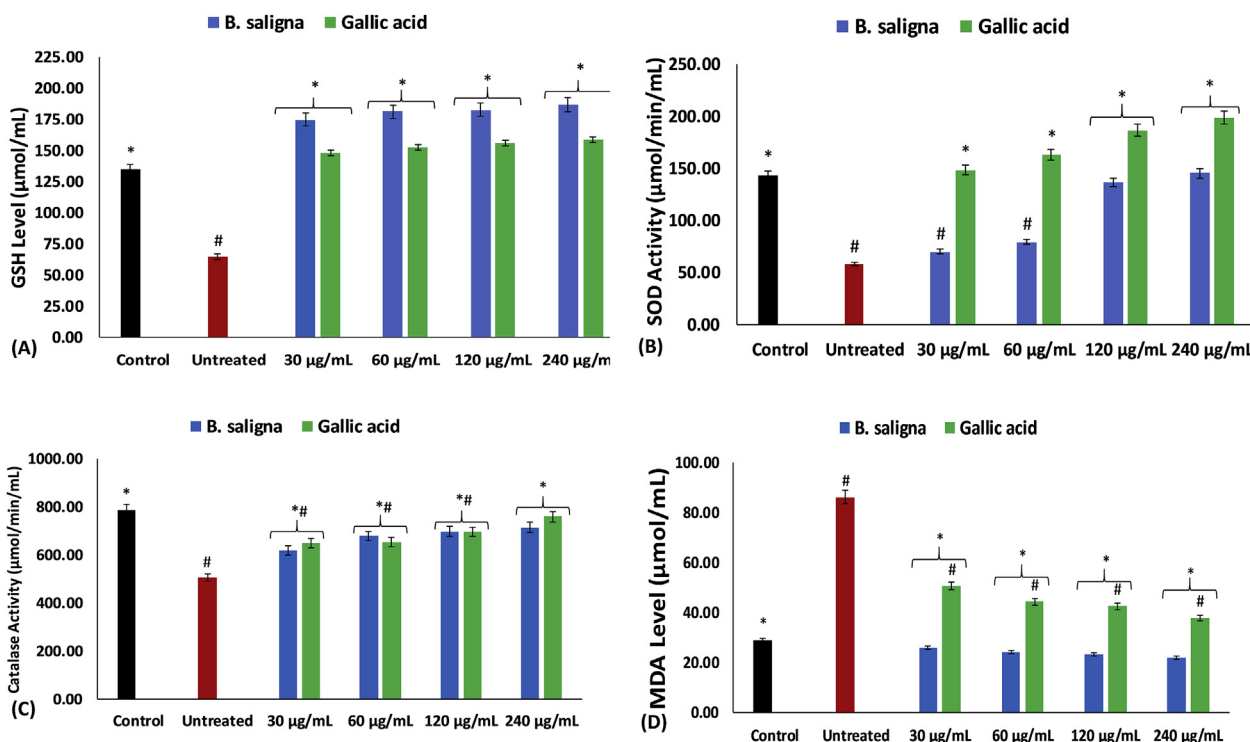
Fig. 1. Effect of *B. saligna* on (A) GSH level, (B) SOD, (C) catalase and (D) MDA level in oxidative cardiopathy. Data = mean ± SD; n = 3. *Statistically significant compared to untreated tissue lysates; #statistically significant compared to normal tissue lysates.
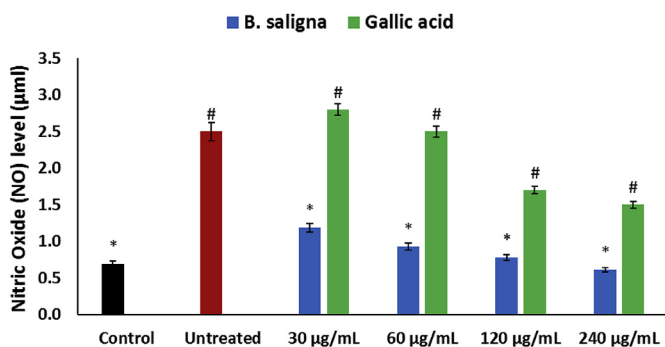

Fig. 2. Effect of *B. saligna* on NO level in oxidative cardiopathy. Data = mean ± SD; n = 3. *Statistically significant compared to untreated tissue lysates; #statistically significant compared to the control (normal tissue lysates).

Fig. 4. Effect of *B. saligna* on acetylcholinesterase activity in oxidative cardiopathy. Data = mean ± SD; n = 3. *Statistically significant compared to untreated tissue lysates; #statistically significant compared to the control (normal tissue lysates).
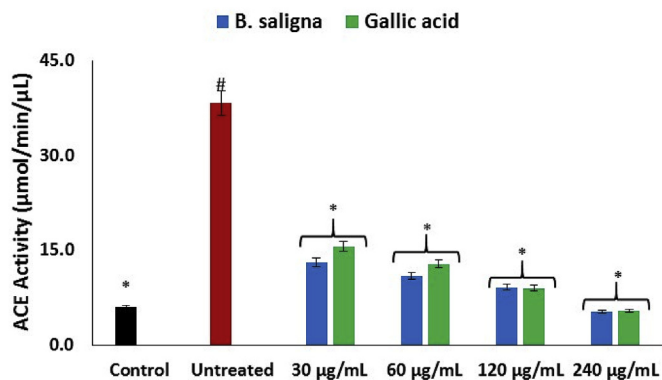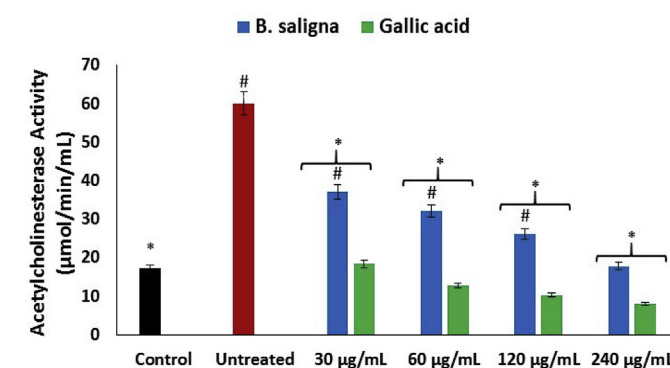

Fig. 3. Effect of *B. saligna* on ACE activity in oxidative cardiopathy. Data = mean ± SD; n = 3. *Statistically significant compared to untreated tissue lysates; #statistically significant compared to the control (normal tissue lysates).

and Zeviani, 1997), with ferric toxicity implicated in its pathogenesis and progression (Albakri, 2018; Gammella et al., 2015). The use of natural products particularly from plant sources in the treatment of cardiovascular dysfunctions and other diseases has been in practice from time immemorial. In the present study, oxidative cardiopathy was induced with ferrous sulphate and treated with *B. saligna*.

Oxidative stress has been implicated in the pathogenesis of cardiopathy and other cardiovascular dysfunctions (Aksakal et al., 2011; Huynh et al., 2014). The depleted levels of GSH, SOD and catalase activities on incubation with $FeSO_4$ (Fig. 1A–C) indicates an occurrence of oxidative damage. This corresponds with previous studies on the reduction of these oxidative biomarkers in cardiovascular dysfunctions (Agunloye et al., 2019). The induction of oxidative stress can be attributed to ferric toxicity via iron-catalyzed Fenton's and Haber Weiss reactions (Latunde-Dada, 2017), which leads to exacerbated generation of superoxide ($O_2^{.-}$). High levels of ($O_2^{.-}$), if not converted to hydrogen peroxide (H_2O_2) by SOD can react with NO to generate the potent
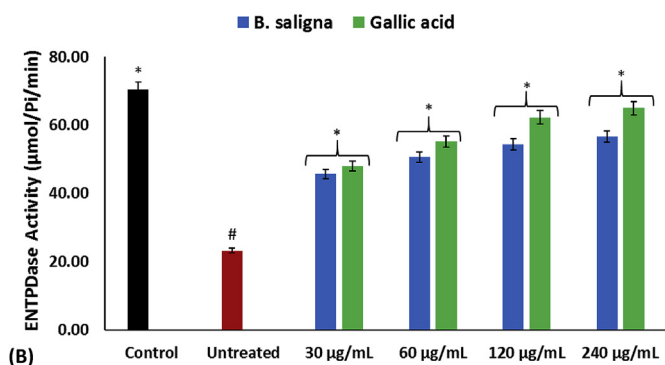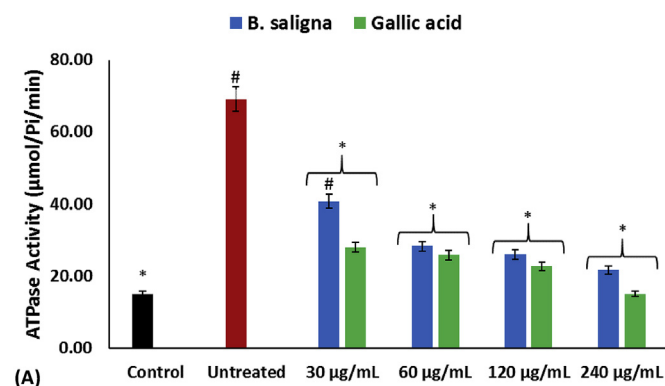
Fig. 5. Effect of *B. saligna* on ATPase and ENTPDase activities in oxidative cardiopathy. Data = mean ± SD; n = 3. *Statistically significant compared to untreated tissue lysates; #statistically significant compared to the control (normal tissue lysates).

Fig. 6. Effect of *B. saligna* on lipase activity in oxidative cardiopathy. Data = mean ± SD; n = 3. *Statistically significant compared to untreated tissue lysates; #statistically significant compared to the control (normal tissue lysates).

Fig. 7. Effect of *B. saligna* on lipid profile in oxidative cardiopathy. Data = mean ± SD; n = 3. *Statistically significant compared to untreated tissue lysates; #statistically significant compared to the control (normal tissue lysates).
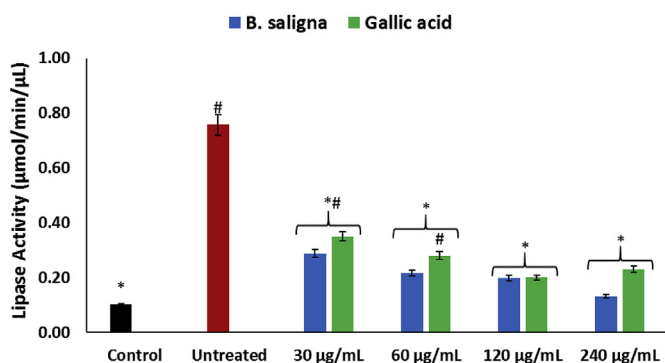
radical, peroxynitrite ($ONOO^-$) which has been implicated in proinflammation. The increased NO level (Fig. 2) and concomitant depleted SOD activity on induction of oxidative stress, therefore insinuates a proinflammatory activity. The elevated MDA level in the untreated tissue (Fig. 1D) portrays an occurrence of lipid peroxidation, which correlates with the depleted catalase activity. The elevated levels of GSH, SOD and catalase activities and concomitant depleted MDA and NO levels on treatment with *B. saligna*, therefore indicates an antioxidative effect on ferric-induced oxidative cardiovascular injury. This corresponds to previous reports on the use of antioxidant in the treatment and management of cardiopathy (Huynh et al., 2014).

Studies have implicated increased ACE activity in the pathogenesis of cardiopathy and other cardiovascular dysfunctions owing to the production and vasoconstrictive effect of angiotensin II (ANG II),
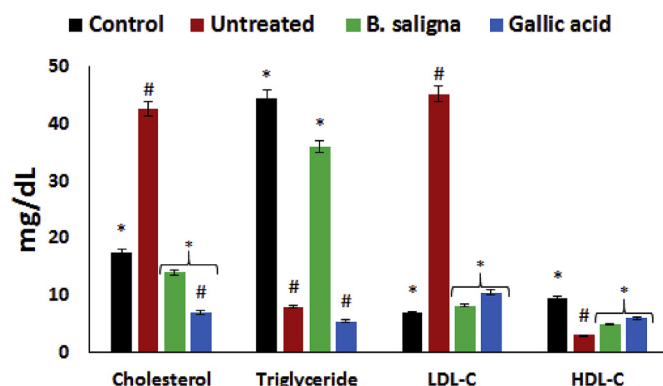
leading to hypertension (Agunloye et al., 2019; Deshmukh et al., 2004; Nikolaidis et al., 2002). The elevated ACE activity in cardiac tissues incubated with $FeSO_4$ (Fig. 3) may further portray a cardiovascular dysfunction on induction of oxidative injury. This corroborates previous reports on the pathogenic role of oxidative stress in the elevation of ACE activity and/or hypertension in cardiopathy (Landmesser and Drexler, 2003; Usui et al., 1999). The depleted activity in the treated cardiac tissues portrays an ACE-inhibitory effect of *B. saligna*, which is further corroborated by the ability of the plant extract to inhibit the activities of ACE and renin in vitro (Figs. S1 and S2, and Table 1). The use of ACE-inhibitors in the treatment and management of cardiovascular dysfunctions has been demonstrated in both basic and clinical studies (Flather et al., 2000; Nikolaidis et al., 2002). Thus, insinuating the therapeutic effect of *B. saligna* on oxidative cardiopathy, which corroborates their use in folkloric medicine for the management of high blood pressure, chest pain and hypertension (Adedapo et al., 2009; Chukwujekwu et al., 2014).

Cholinergic dysfunction contributes to cardiopathy and other cardiovascular dysfunctions as acetylcholine mediates cholinergic-induced vasodilation by activating the muscarinic receptors (Kellogg et al., 2005). The elevated acetylcholinesterase activity on induction of oxidative stress (Fig. 4) indicates a cholinergic dysfunction, as acetylcholinesterase hydrolyzes acetylcholine which suppresses its availability to mediate vasodilation of the cardiac muscles (Agunloye et al., 2019). This is evident in the use of acetylcholine-inhibitors as effective therapy in the treatment and management of cardiovascular dysfunctions (Gavioli et al., 2014; Roy et al., 2014; Wu et al., 2017). The depleted activity in the treated tissues thus indicates a modulatory and therapeutic effect of *B. saligna* on cardiac cholinergic dysfunction.

The endogenous signaling nucleotide, adenosine plays an important role in cardiac functions as it acts as a powerful dilator of the coronary vessels (Burnstock, 2017; Burnstock and Ralevic, 2014). Adenosine has also been reported to mitigate the myocardial effect of catecholamines (Burnstock, 2017). The elevated cardiac activity of ATPase and concomitant depleted ENTPDase activity on induction of oxidative stress (Fig. 5A and B) indicates a decreased level of ATP and adenosine, respectively. Increased ATP level has been demonstrated to mitigate hypertension by acting on P2 receptors on endothelial cells to release NO, leading to vasodilation which causes decreased blood pressure (Burnstock, 2017; Burnstock and Ralevic, 2014; Wang et al., 2015). The depleted ATPase and ENTPDase activities in cardiac tissues treated with *B. saligna* indicates an increased ATP level available for hydrolysis to adenosine. It may also insinuate availability of ATP to mitigate hypertension by decreasing blood pressure via the actions on P2 receptors.

The importance of lipase activity in the availability of fatty acids (FA) to the cardiac tissue has been reported (Pulinilkunnil and

Table 2
GC-MS identified fatty acid metabolites in experimental cardiac tissue lysates.

	Metabolites	Normal	Untreated	Treated
Fatty alkane	Eicosane	2.35 ± 0.42	1.89 ± 0.30	3.36 ± 0.7
Fatty alkene	Squalene	ND	0.24 ± 0.05	ND
Fatty acyl	n-Tetradecane	1.34 ± 0.20	1.13 ± 0.15	ND
	2,3,6-Trimethyldecane	1.81 ± 0.30	ND	ND
	2,6,10,15-Tetramethylheptadecane	3.99 ± 0.66	4.35 ± 0.76	3.61 ± 0.68
Fatty alcohol	Pentadecanol	0.4 ± 0.03	0.39 ± 0.06	0.36 ± 0.01
	n-Heptadecanol-1	0.92 ± 0.07	0.83 ± 0.05	0.7 ± 0.07
	n-Tetracosanol-1	0.32 ± 0.001	0.47 ± 0.03	ND
Fatty acid	Tetrahydroionol	ND	ND	0.14 ± 0.01
	Pentadecanoic acid	6.27 ± 0.33	0.27 ± 0.03	ND
	cis-9, cis-12-Octadecadienoic acid	3.67 ± 0.12	4.66 ± 0.4	0.98 ± 0.135
	Palmitoleic acid	2.01 ± 0.18	2.78 ± 0.17	ND
	cis-10-Heptadecenoic acid	0.97 ± 0.1	5.57 ± 0.23	ND
	Octadecanoic acid	5.29 ± 0.1	5.4 ± 0.02	1.75 ± 0.14
	Tetracosanoic acid	ND	0.51 ± 0.07	ND
	Palmitic acid	ND	6.73 ± 0.87	ND
	Arachidonic acid	0.88 ± 0.08	1.22 ± 0.10	ND
	9-Octadecenoic acid, (E)-	ND	1.63 ± 0.29	ND
	Nonahexacontanoic acid	ND	ND	0.33 ± 0.04
	2-Dodecenoic acid	ND	ND	0.13 ± 0.005
Fatty acid ester	Pentadecanoic acid, ethyl ester	3.38 ± 0.43	ND	ND
	Ethyl palmitate	1.51 ± 0.24	1.31 ± 0.21	1.83 ± 0.33
	Arachidic acid, ethyl ester	ND	2.93 ± 0.35	0.2 ± 0.02
	Allyl decanoate	ND	ND	0.19 ± 0.01
	l-(+)-Ascorbic acid 2,6-dihexadecanoate	ND	ND	2.14 ± 0.30
Glycerol	Glycerol 1-palmitate	ND	0.53 ± 0.03	ND
Fatty amide	Oleyl amide	ND	ND	0.22 ± 0.03
Glycol	1-O-(22-Hydroxydocosyl)-d-mannitol	0.63 ± 0.02	ND	ND
Steroids	Cholesterol	1.05 ± 0.02	3.36 ± 0.10	0.78 ± 0.11
	(11.alpha.)-11-Methoxypregn-4-ene-3,20-dione	ND	ND	0.15 ± 0.02
	25-Hydroxycholesterol, dimethyl ether	ND	ND	0.54 ± 0.04
	2,2-Dimethoxycholestane	ND	ND	0.18 ± 0.01
Non-lipid	Retinal	0.63 ± 0.02	ND	ND
	R1-Barrigenol	ND	ND	0.25 ± 0.09
	24,25-Dihydroxyvitamin D	ND	ND	0.38 ± 0.02
	Cymarin	ND	ND	0.26 ± 0.01
	alpha-Terpineol	ND	ND	0.38 ± 0.01

Data = mean ± SD; n = 3. ND = not detected.

Rodrigues, 2006; Rodrigues et al., 1992). It catalyzes the lipolysis of cardiac triglyceride (TG) (endogenous store or exogenous sources) to FA, as the ability of the heart to synthesize FA is limited (Pulinilkunnil and Rodrigues, 2006). Chronic exacerbated activity has been implicated in abnormal cardiac FA level and utilization which could lead to cardiovascular dysfunction (Lee et al., 2004; Pulinilkunnil and Rodrigues, 2006). Therefore, the elevated lipase activity in cardiac tissues on activation of oxidative stress (Fig. 6) indicates an abnormality in FA
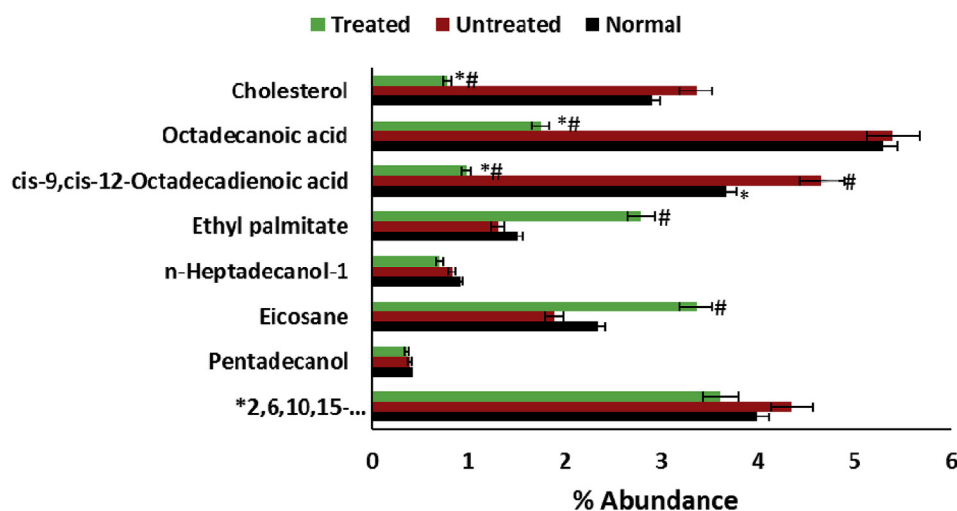
Fig. 8. Common lipid metabolites in experimental cardiac tissue lysates. Data = mean ± SD; n = 3. *Statistically significant compared to untreated tissue lysates; #statistically significant compared to normal tissue lysates. *2,6,10,15-Tetramethylheptadecane.
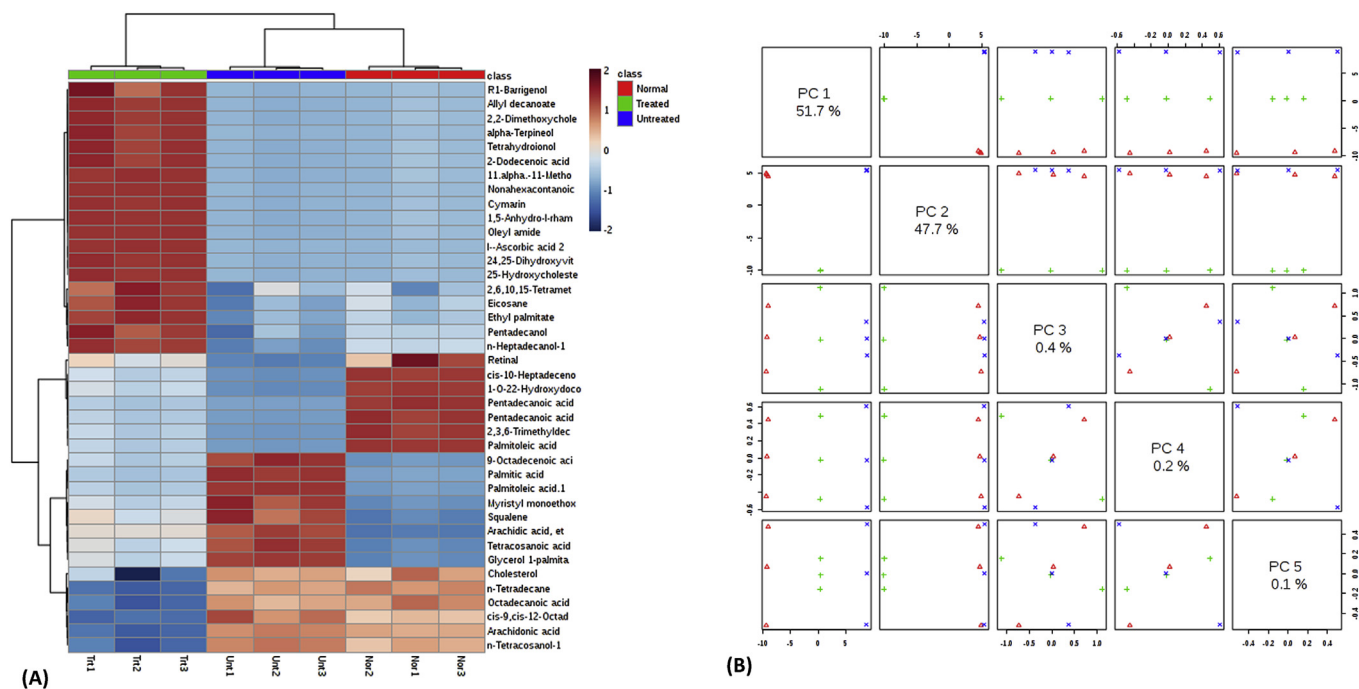
Fig. 9. (A) Heat map; and (B) PC scores of the identified fatty acid metabolites. Nor = normal; Unt = untreated; and Trt: treated tissue lysates.

supply and utilization that portrays a lipotoxic effect. The depleted activity in cardiac tissues treated with *B. saligna* suggests a modulatory effect on cardiac accumulation and utilization of FA.

The role of cholesterol and triglycerides in the pathogenesis of cardiac dysfunctions is well documented. Disruption of the cardiac lipid spectrum characterized by exacerbated levels of these lipids as well as depleted HDL-c level has been implicated in the proliferation of cardiopathy (Poulter, 2003). High cellular levels of cholesterols and LDL-c have also been linked to increased vasoconstriction, thereby contributing to high blood pressure and hypertension (Kopkan et al., 2009; Rosendorff, 2002). The elevated levels of cholesterol, LDL-c and depleted HDL-c level on induction of oxidative stress (Fig. 7) portrays a disrupted cardiac lipid spectrum which insinuates a hyperlipidemic effect. The depleted triglyceride level on induction of oxidative stress can be attributed to the increased lipase activity (Fig. 6), insinuating its utilization for FA production (Pulinilkunnil and Rodrigues, 2006). The depleted levels of cholesterol and LDL-c, and elevated HDL-c level in the treated cardiac tissues indicates a therapeutic effect of *B. saligna* on oxidative disrupted cardiac lipid spectrum.

Disturbances in cardiac lipid metabolism characterized by accumulation of free fatty acids (FFAs) and hyperlipidemia leading to

defects in energy metabolism have been recognized as a major mechanism of cardiopathies (Antozzi and Zeviani, 1997; Ventura-Clapier et al., 2004). The elevated lipid concentrations particularly cholesterol, squalene, tetracosanoic acid, palmitic acid, glycerol 1-palmitate and 9-Octadecenoic acid, (E)- (Figs. 8 and 9, and Table 2) on induction of oxidative stress portrays an alteration in the cardiac lipid contents and concentrations. This corroborates the elevated lipase activity in oxidative injured cardiac tissues (Fig. 6). The presence of tetracosanoic acid and palmitic acid denotes an increased level of saturated fatty acids, which may pose a lipotoxic effect as high concentrations of saturated fatty acids have been implicated in vasoconstrictions leading to high blood pressure and cardiac dysfunction (Dow et al., 2014). 9-Octadecenoic acid, (E)- has also been linked to increased LDL-c and depleted HDL-c levels (Abbey and Nestel, 1994). The reduced cholesterol level and total depletion of squalene, tetracosanoic acid, palmitic acid, glycerol 1-palmitate and 9-Octadecenoic acid, (E)- in cardiac tissues treated with *B. saligna* depicts a modulatory effect on cardiac lipid accumulation, which correlates with the decreased lipase activity. The presence of oleyl amide further denotes the cardio-protective effect of the extract, as the fatty amide has been linked to myocardial development and vasodilation (Hiley and Hoi, 2007). The presence of the
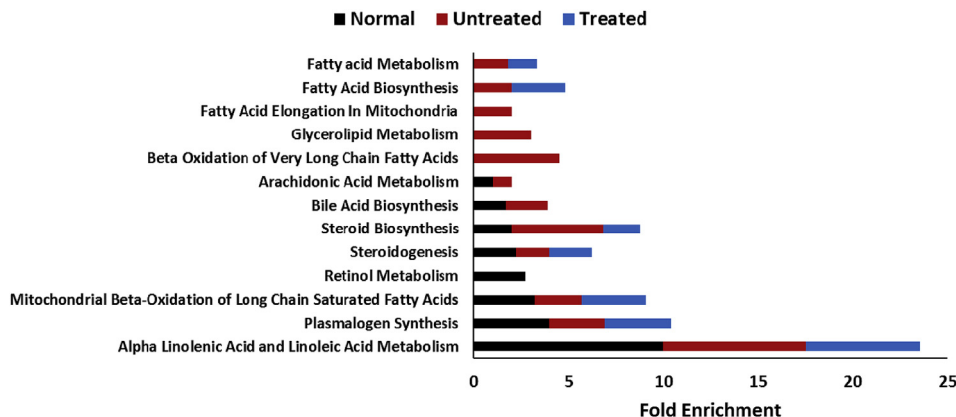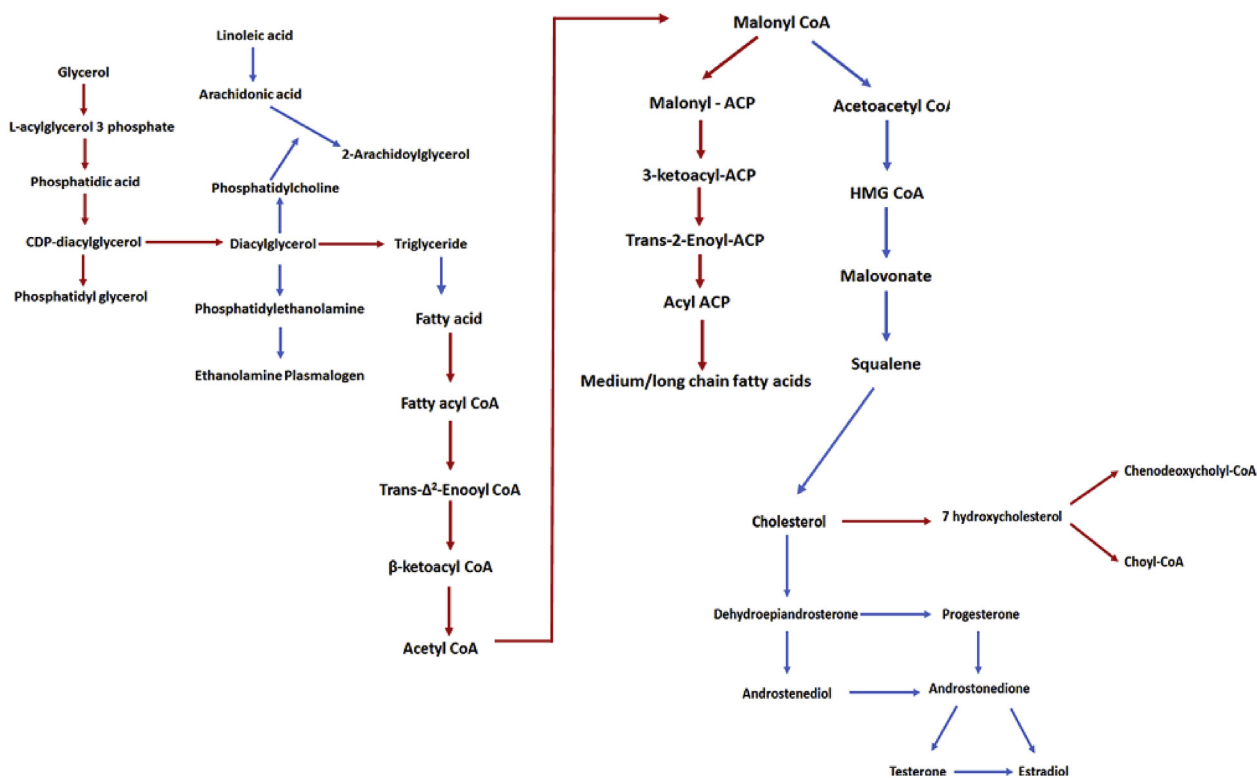

Fig. 10. Fold enrichment of identified lipid metabolic pathways.

Fig. 11. Schematic network of the most relevant metabolic pathways in the studied cardiac tissues. Red arrows indicate pathways activated on induction of oxidative injury. Blue arrows depict pathways common to normal and treated tissues. (For interpretation of the references to colour in this figure legend, the reader is referred to the Web version of this article.)

Table 3
Retention times and percentage peak areas of HPLC-identified polyphenols in the MeOH: DCM extract of *B. saligna*.

Polyphenols	Parameters	Extract
Methyl gallate (RT: 13.810 min)	RT (min)	13.709
	DFS (min)	−0.101
	Peak area (%)	1.6129%
Ferulic acid (RT: 19.937 min)	RT (min)	19.711
	DFS (min)	−0.226
	Peak area (%)	7.4178%
Quercetin (RT: 25.210 min)	RT (min)	25.245
	DFS (min)	+0.035
	Peak area (%)	7.1035%

RT: Peak Retention time; DFS: The difference between the peak retention time of the extract and standard.

antioxidant biomarkers l-(+)-Ascorbic acid 2,6-dihexadecanoate and 24,25-Dihydroxyvitamin D also depicts the antioxidant activity of the plant on oxidative cardiopathy. The modulatory effects of cholesterol metabolites, particularly 25-hydroxycholesterol, dimethyl ether on cholesterol esterification and transportation to the endoplasmic reticulum has been reported (Du et al., 2004). Thus, their presence in the treated tissues insinuates a hypocholesteremic potential of *B. saligna* which also correlates with the decreased cholesterol level (Figs. 7 and 8, Table 2).

Defects in mitochondrial oxidative metabolism comprising oxidative phosphorylation and β-oxidation have reported as the major energy dysmetabolism in cardiopathies (Antozzi and Zeviani, 1997). The activation of pathways for beta oxidation of very long chain fatty acids, glycerolipid metabolism, fatty acid elongation in mitochondria, fatty acid biosynthesis and fatty acid metabolism on induction of oxidative injury (Figs. 10 and 11) denotes an increased metabolism of FFA, which

may be attributed to the breakdown of triglyceride by lipase (Evans and Hauton, 2016). Thus, correlating with the increased lipase activity and depleted triglyceride level. Activation of these metabolic pathways implies an increased production of the electron donors, NADH and FADH$_2$ as well as the end product, acetyl-CoA (Marín-Garcí;a and Goldenthal, 2002). The latter enters the tricarboxylic acid (TCA) cycle and further oxidized to CO_2 while yet generating NADH, FADH$_2$ and ATP. The generated NADH and FADH$_2$ then enters the respiratory chain and utilized in the production of ATP. The increased production of these electron donors would lead to inhibition of the electron transport at complex II, owing to the generation of a high mitochondrial membrane potential (Brownlee, 2001; Du et al., 2001). Thereby, concomitantly reducing oxygen to (O_2) to $O_2^{\cdot-}$ (Brownlee, 2001). The continuous generation of $O_2^{\cdot-}$ in the presence of reduced SOD activity (Fig. 1B) and elevated NO level (Fig. 2) would lead to oxidative stress. The inactivation of pathways for beta oxidation of very long chain fatty acids, glycerolipid metabolism and fatty acid elongation in mitochondria in cardiac tissues treated with *B. saligna* depicts a decreased production of the electron carriers. Thus, implying a decreased generation of $O_2^{\cdot-}$ and subsequently suppressing oxidative stress. The inactivated bile acid biosynthesis pathway further depicts the cardio-protective potential of *B. saligna* as the cardio-regulatory and vasoconstrictive effects of bile acids have been reported (Khurana et al., 2011; Lofthouse et al., 2019; Sepulveda et al., 1991).

These activities of *B. saligna* may be attributed to the synergistic effects of its phytochemical constituents, particularly the HPLC-identified phenolics of the extract: methyl gallate, ferulic acid and quercetin (Table 3). Phenolics have been reported for their antioxidative, antihypertensive and cardioprotective effects (Agunloye et al., 2019; Erukainure et al., 2018). The antihypertensive activity of methyl gallate and its derivatives has been demonstrated *in vitro* and *in vivo* (Kurita et al., 2010). Ferulic acid has been reported for its ability to restore endothelial function via enhancement of basal and stimulated NO

bioavailability in aortas (Suzuki et al., 2007; Zhao et al., 2012). While the ability of quercetin to suppress systolic blood pressure and plasma oxidized LDL levels has been demonstrated in overweight subjects with high-cardiovascular disease (Egert et al., 2009). Decreased incidences of cerebrovascular disease have also been correlated with increased quercetin intake (Knekt et al., 2000).

5. Conclusion

In summary, these results suggest the protective effects of *B. saligna* on ferric-induced oxidative cardiopathy as demonstrated by its ability to mitigate oxidative stress, while inhibiting the enzymatic activities of ACE, acetylcholinesterase and lipase, and concomitantly modulating cardiac lipid spectrum and dysregulated metabolic pathways. Thereby, giving credence to its traditional use in the treatment and management of cardio-dysfunctional related ailments. These activities may be attributed to the synergistic effect of the identified phenolics. However, *in vivo* and clinical studies will be required to further decipher its possible molecular mechanisms.

Declaration of competing interest

The authors declare no conflict of interests.

Acknowledgments

Appendix A. Supplementary data

Supplementary data to this article can be found online at https://doi.org/10.1016/j.jep.2019.112358.

Authors contribution

MGM, CIC and OLE conceptualized the research idea; CIC and MGM carried out the *in vitro* and HPLC studies; OLE, VFS and MSI carried out the *ex vivo* studies; NAK and OLE carried out the LCMS analysis; OLE carried out the metabolic studies; OLE and CIC drafted the manuscript; all authors read and approved the manuscript.

References

Abbey, M., Nestel, P.J., 1994. Plasma cholesteryl ester transfer protein activity is increased when trans-elaidic acid is substituted for cis-oleic acid in the diet. Atherosclerosis 106 (1), 99–107.

Adedapo, A.A., Jimoh, F.O., Koduru, S., Masika, P.J., Afolayan, A.J., 2009. Assessment of the medicinal potentials of the methanol extracts of the leaves and stems of Buddleja saligna. BMC Complement Altern. Med. 9 (1), 21.

Adewoye, O., Bolarinwa, A., Olorunsogo, O., 2000. Ca + +, Mg + +-ATPase activity in insulin-dependent and non-insulin dependent diabetic Nigerians. Afr. J. Med. Med. Sci. 29 (3–4), 195–199.

Aebi, H., 1984. Catalase in vitro. Methods Enzymol. 105, 121–126.

Agunloye, O.M., Oboh, G., Ademiluyi, A.O., Ademosun, A.O., Akindahunsi, A.A., Oyagbemi, A.A., Omobowale, T.O., Ajibade, T.O., Adedapo, A.A., 2019. Cardio-protective and antioxidant properties of caffeic acid and chlorogenic acid: Mechanistic role of angiotensin converting enzyme, cholinesterase and arginase activities in cyclosporine induced hypertensive rats. Biomed. Pharmacother. 109, 450–458.

Akomolafe, S., Akinyemi, A., Ogunsuyi, O., Oyeleye, S., Oboh, G., Adeoyo, O., Allismith, Y., 2017. Effect of caffeine, caffeic acid and their various combinations on enzymes of cholinergic, monoaminergic and purinergic systems critical to neurodegeneration in rat brain—in vitro. NeuroToxicology 62, 6–13.

Aksakal, E., Akaras, N., Kurt, M., Tanboga, I., Halici, Z., Odabasoglu, F., Bakirci, E., Unal, B., 2011. The role of oxidative stress in diabetic cardiomyopathy: an experimental study. Eur. Rev. Med. Pharmacol. Sci. 15 (11), 1241–1246.

Albakri, A., 2018. Iron overload cardiomyopathy: a review of literature on clinical status and meta-analysis of diagnostic and clinical management using iron chelators. Intern. Med. Care. 2 (1), 1–12.

Antozzi, C., Zeviani, M., 1997. Cardiomyopathies in disorders of oxidative metabolism. Cardiovasc. Res. 35 (2), 184–199.

Aubrey, A., 2002. Buddleja saligna Willd. http://pza.sanbi.org/buddleja-saligna, Accessed date: 1 September 2019.

Brownlee, M., 2001. Biochemistry and molecular cell biology of diabetic complications. Nature 414 (6865), 813.

Burnstock, G., 2017. Purinergic signaling in the cardiovascular system. Circ. Res. 120 (1), 207–228.

Burnstock, G., Ralevic, V., 2014. Purinergic signaling and blood vessels in health and disease. Pharmacol. Rev. 66 (1), 102–192.

Chong, J., Soufan, O., Li, C., Caraus, I., Li, S., Bourque, G., Wishart, D.S., Xia, J., 2018. MetaboAnalyst 4.0: towards more transparent and integrative metabolomics analysis. Nucleic Acids Res. 46 (W1), W486–W494.

Chowdhury, P., Soulsby, M., 2002. Lipid peroxidation in rat brain is increased by simulated weightlessness and decreased by a soy-protein diet. Ann. Clin. Lab. Sci. 32 (2), 188–192.

Chukwujekwu, J.C., Amoo, S.O., de Kock, C.A., Smith, P.J., Van Staden, J., 2014. Antiplasmodial, acetylcholinesterase and alpha-glucosidase inhibitory and cytotoxicity properties of Buddleja saligna. South Afr. J. Bot. 94, 6–8.

Chukwujekwu, J.C., Rengasamy, K.R., de Kock, C.A., Smith, P.J., Slavětínská, L.P., van Staden, J., 2016. Alpha-glucosidase inhibitory and antiplasmodial properties of terpenoids from the leaves of Buddleja saligna Willd. J. Enzym. Inhib. Med. Chem. 31 (1), 63–66.

Chukwuma, C.I., Matsabisa, M.G., Ibrahim, M.A., Erukainure, O.L., Chabalala, M.H., Islam, M.S., 2019. Medicinal plants with concomitant anti-diabetic and anti-hypertensive effects as potential sources of dual acting therapies against diabetes and hypertension: a review. J. Ethnopharmacol. 235, 329–360.

De Blasio, M.J., Huynh, K., Qin, C., Rosli, S., Kiriazis, H., Ayer, A., Cemerlang, N., Stocker, R., Du, X.-J., McMullen, J.R., 2015. Therapeutic targeting of oxidative stress with coenzyme Q10 counteracts exaggerated diabetic cardiomyopathy in a mouse model of diabetes with diminished PI3K (p110α) signaling. Free Radic. Biol. Med. 87, 137–147.

Deshmukh, P.M., Krishnamani, R., Romanyshyn, M., Johnson, A.K., Noti, J.D., 2004. Association of angiotensin converting enzyme gene polymorphism with tachycardia cardiomyopathy. Int. J. Mol. Med. 13 (3), 455–458.

Dow, C.A., Stauffer, B.L., Greiner, J.J., DeSouza, C.A., 2014. Influence of dietary saturated fat intake on endothelial fibrinolytic capacity in adults. Am. J. Cardiol. 114 (5), 783–788.

Du, X., Pham, Y.H., Brown, A.J., 2004. Effects of 25-Hydroxycholesterol on cholesterol esterification and sterol regulatory element-binding protein processing are dissociable implications for cholesterol movement to the regulatory pool in the endoplasmic reticulum. J. Biol. Chem. 279 (45), 47010–47016.

Du, X.L., Edelstein, D., Dimmeler, S., Ju, Q., Sui, C., Brownlee, M., 2001. Hyperglycemia inhibits endothelial nitric oxide synthase activity by posttranslational modification at the Akt site. J. Clin. Investig. 108 (9), 1341–1348.

Egert, S., Bosy-Westphal, A., Seiberl, J., Kürbitz, C., Settler, U., Plachta-Danielzik, S., Wagner, A.E., Frank, J., Schrezenmeir, J., Rimbach, G., 2009. Quercetin reduces systolic blood pressure and plasma oxidised low-density lipoprotein concentrations in overweight subjects with a high-cardiovascular disease risk phenotype: a double-blinded, placebo-controlled cross-over study. Br. J. Nutr. 102 (7), 1065–1074.

Ellman, G.L., 1959. Tissue sulfhydryl groups. Arch. Biochem. Biophys. 82 (1), 70–77.

Ellman, G.L., Courtney, K.D., Andres Jr., V., Featherstone, R.M., 1961. A new and rapid colorimetric determination of acetylcholinesterase activity. Biochem. Pharmacol. 7 (2), 88–95.

Erukainure, O.L., Hafizur, R., Kabir, N., Choudhary, I., Atolani, O., Banerjee, P., Preissner, R., Chukwuma, C.I., Muhammad, A., Amonsou, E., 2018. Suppressive effects of clerodendrum volubile P beauv.[labiatae] methanolic extract and its fractions on type 2 diabetes and its complications. Front. Pharmacol. 9, 8.

Erukainure, O.L., Mopuri, R., Oyebode, O.A., Koorbanally, N.A., Islam, M.S., 2017a. Dacryodes edulis enhances antioxidant activities, suppresses DNA fragmentation in oxidative pancreatic and hepatic injuries; and inhibits carbohydrate digestive enzymes linked to type 2 diabetes. Biomed. Pharmacother. 96, 37–47.

Erukainure, O.L., Oyebode, O.A., Ibeji, C.U., Koorbanally, N.A., Islam, M.S., 2019. Vernonia Amygdalina Del. stimulated glucose uptake in brain tissues enhances antioxidative activities; and modulates functional chemistry and dysregulated metabolic pathways. Metab. Brain Dis. 34, 721–732.

Erukainure, O.L., Oyebode, O.A., Sokhela, M.K., Koorbanally, N.A., Islam, M.S., 2017b. Caffeine–rich infusion from Cola nitida (kola nut) inhibits major carbohydrate catabolic enzymes; abates redox imbalance; and modulates oxidative dysregulated metabolic pathways and metabolites in Fe 2 +-induced hepatic toxicity. Biomed. Pharmacother. 96, 1065–1074.

Evans, R.D., Hauton, D., 2016. The role of triacylglycerol in cardiac energy provision. Biochim. Biophys. Acta Mol. Cell Biol. Lipids 1861 (10), 1481–1491.

Flather, M.D., Yusuf, S., Køber, L., Pfeffer, M., Hall, A., Murray, G., Torp-Pedersen, C., Ball, S., Pogue, J., Moyé, L., 2000. Long-term ACE-inhibitor therapy in patients with heart failure or left-ventricular dysfunction: a systematic overview of data from

individual patients. Lancet 355 (9215), 1575–1581.

Gammella, E., Recalcati, S., Rybinska, I., Buratti, P., Cairo, G., 2015. Iron-induced damage in cardiomyopathy: oxidative-dependent and independent mechanisms. Oxid. Med. Cell. Longev. 2015, 230182.

Gavioli, M., Lara, A., Almeida, P.W., Lima, A.M., Damasceno, D.D., Rocha-Resende, C., Ladeira, M., Resende, R.R., Martinelli, P.M., Melo, M.B., 2014. Cholinergic signaling exerts protective effects in models of sympathetic hyperactivity-induced cardiac dysfunction. PLoS One 9 (7), e100179.

Hiley, C.R., Hoi, P.M., 2007. Oleamide: a fatty acid amide signaling molecule in the cardiovascular system? Cardiovasc. Drug Rev. 25 (1), 46–60.

Holmquist, B., Bünning, P., Riordan, J.F., 1979. A continuous spectrophotometric assay for angiotensin converting enzyme. Anal. Biochem. 95 (2), 540–548.

Huynh, K., Bernardo, B.C., McMullen, J.R., Ritchie, R.H., 2014. Diabetic cardiomyopathy: mechanisms and new treatment strategies targeting antioxidant signaling pathways. Pharmacol. Ther. 142 (3), 375–415.

Huynh, K., Kiriazis, H., Du, X.-J., Love, J.E., Gray, S.P., Jandeleit-Dahm, K.A., McMullen, J.R., Ritchie, R.H., 2013. Targeting the upregulation of reactive oxygen species subsequent to hyperglycemia prevents type 1 diabetic cardiomyopathy in mice. Free Radic. Biol. Med. 60, 307–317.

Jaradat, N.A., 2005. Medical plants utilized in Palestinian folk medicine for treatment of diabetes mellitus and cardiac diseases. J. Al-Aqsa. Univ. 9, 1–28.

Kakkar, P., Das, B., Viswanathan, P., 1984. A modified spectrophotometric assay of superoxide dismutase. Indian J. Biochem. Biophys. 21, 130–132.

Kellogg Jr., D.L., Zhao, J., Coey, U., Green, J., 2005. Acetylcholine-induced vasodilation is mediated by nitric oxide and prostaglandins in human skin. J. Appl. Physiol. 98 (2), 629–632.

Khurana, S., Raufman, J.P., Pallone, T.L., 2011. Bile acids regulate cardiovascular function. Clin. Transl. Sci. 4 (3), 210–218.

Kim, Y.S., Lee, Y.M., Kim, H., Kim, J., Jang, D.S., Kim, J.H., Kim, J.S., 2010. Anti-obesity effect of Morus bombycis root extract: anti-lipase activity and lipolytic effect. J. Ethnopharmacol. 130 (3), 621–624.

Knekt, P., Isotupa, S., Rissanen, H., Heliövaara, M., Järvinen, R., Häkkinen, S., Aromaa, A., Reunanen, A., 2000. Quercetin intake and the incidence of cerebrovascular disease. Eur. J. Clin. Nutr. 54 (5), 415.

Kopkan, L., Khan, M.A.H., Lis, A., Awayda, M.S., Majid, D.S., 2009. Cholesterol induces renal vasoconstriction and anti-natriuresis by inhibiting nitric oxide production in anesthetized rats. Am. J. Physiol-Renal. 297 (6), F1606–F1613.

Kovacic, P., Thurn, L.A., 2005. Cardiovascular toxicity from the perspective of oxidative stress, electron transfer, and prevention by antioxidants. Curr. Vasc. Pharmacol. 3 (2), 107–117.

Kurita, I., Maeda-Yamamoto, M., Tachibana, H., Kamei, M., 2010. Antihypertensive effect of Benifuuki tea containing O-methylated EGCG. J. Agric. Food Chem. 58 (3), 1903–1908.

Landmesser, U., Drexler, H., 2003. Oxidative stress, the renin-angiotensin system, and atherosclerosis. Eur. Heart J. Suppl. 5 (Suppl. l_A), A3–A7.

Latunde-Dada, G.O., 2017. Ferroptosis: role of lipid peroxidation, iron and ferritinophagy. Biochim. Biophys. Acta Gen. Subj. 1861 (8), 1893–1900.

Lee, Y., Naseem, R.H., Duplomb, L., Park, B.-H., Garry, D.J., Richardson, J.A., Schaffer, J.E., Unger, R.H., 2004. Hyperleptinemia prevents lipotoxic cardiomyopathy in acyl CoA synthase transgenic mice. Proc. Natl. Acad. Sci. 101 (37), 13624–13629.

Lofthouse, E.M., Torrens, C., Manousopoulou, A., Nahar, M., Cleal, J.K., O'Kelly, I.M., Sengers, B.G., Garbis, S.D., Lewis, R.M., 2019. Ursodeoxycholic acid inhibits uptake and vasoconstrictor effects of taurocholate in human placenta. FASEB J. 33 (7), 8211–8220.

Marín-García, J., Goldenthal, M.J., 2002. Fatty acid metabolism in cardiac failure: biochemical, genetic and cellular analysis. Cardiovasc. Res. 54 (3), 516–527.

Mashour, N.H., Lin, G.I., Frishman, W.H., 1998. Herbal medicine for the treatment of

cardiovascular disease: clinical considerations. Arch. Intern. Med. 158 (20), 2225–2234.

Nikolaidis, L.A., Doverspike, A., Huerbin, R., Hentosz, T., Shannon, R.P., 2002. Angiotensin-converting enzyme inhibitors improve coronary flow reserve in dilated cardiomyopathy by a bradykinin-mediated, nitric oxide-dependent mechanism. Circulation 105 (23), 2785–2790.

Poulter, N., 2003. Global risk of cardiovascular disease. Heart 89 (Suppl. 2), ii2–ii5.

Pulinilkunnil, T., Rodrigues, B., 2006. Cardiac lipoprotein lipase: metabolic basis for diabetic heart disease. Cardiovasc. Res. 69 (2), 329–340.

Ralston-Hooper, K., Jannasch, A., Adamec, J., Sepúlveda, M., 2011. The use of two-dimensional gas chromatography–time-of-flight mass spectrometry (gc × gc–tof-ms) for metabolomic analysis of polar metabolites. In: Metz, T.O. (Ed.), Metabolic Profiling. Springer, pp. 205–211.

Rodrigues, B., Braun, J.E., Spooner, M., Severson, D.L., 1992. Regulation of lipoprotein lipase activity in cardiac myocytes from control and diabetic rat hearts by plasma lipids. Can. J. Physiol. Pharmacol. 70 (9), 1271–1279.

Rosendorff, C., 2002. Effects of LDL cholesterol on vascular function. J. Hum. Hypertens. 16 (S1), S26.

Roy, A., Guatimosim, S., Prado, V.F., Gros, R., Prado, M.A., 2014. Cholinergic activity as a new target in diseases of the heart. Mol. Med. 20 (1), 527.

Sepulveda, W., Gonzalez, C., Cruz, M., Rudolph, M., 1991. Vasoconstrictive effect of bile acids on isolated human placental chorionic veins. Eur. J. Obstet. Gynecol. Reprod. Biol. 42 (3), 211–215.

Shalaby, S.M., Zakora, M., Otte, J., 2006. Performance of two commonly used angiotensin-converting enzyme inhibition assays using FA-PGG and HHL as substrates. J. Dairy Res. 73 (2), 178–186.

Shirpoor, A., Salami, S., Khadem-Ansari, M.H., Ilkhanizadeh, B., Pakdel, F.G., Khademvatani, K., 2009. Cardioprotective effect of vitamin E: rescues of diabetes-induced cardiac malfunction, oxidative stress, and apoptosis in rat. J. Diabetes Complicat. 23 (5), 310–316.

Suzuki, A., Yamamoto, M., Jokura, H., Fujii, A., Tokimitsu, I., Hase, T., Saito, I., 2007. Ferulic acid restores endothelium-dependent vasodilation in aortas of spontaneously hypertensive rats. Am. J. Hypertens. 20 (5), 508–513.

Tsikas, D., 2005. Review Methods of quantitative analysis of the nitric oxide metabolites nitrite and nitrate in human biological fluids. Free Radic. Res. 39 (8), 797–815.

Usui, M., Egashira, K., Kitamoto, S., Koyanagi, M., Katoh, M., Kataoka, C., Shimokawa, H., Takeshita, A., 1999. Pathogenic role of oxidative stress in vascular angiotensin-converting enzyme activation in long-term blockade of nitric oxide synthesis in rats. Hypertension (Dallas) 34 (4), 546–551.

Ventura-Clapier, R., Garnier, A., Veksler, V., 2004. Energy metabolism in heart failure. J. Physiol. 555 (1), 1–13.

Wang, S., Iring, A., Strilic, B., Juárez, J.A., Kaur, H., Troidl, K., Tonack, S., Burbiel, J.C., Müller, C.E., Fleming, I., 2015. P2Y 2 and G q/G 11 control blood pressure by mediating endothelial mechanotransduction. J. Clin. Investig. 125 (8), 3077–3086.

Wojciechowska, C., Romuk, E., Tomasik, A., Skrzep-Poloczek, B., Nowalany-Kozielska, E., Birkner, E., Jacheć, W., 2014. Oxidative stress markers and C-reactive protein are related to severity of heart failure in patients with dilated cardiomyopathy. Mediat. Inflamm. 2014, 147040.

Wold, L.E., CEYLAN-ISIK, A.F., Ren, J., 2005. Oxidative stress and stress signaling: menace of diabetic cardiomyopathy. Acta Pharmacol. Sin. 26 (8), 908–917.

Wu, S.J., Li, Y.C., Shi, Z.W., Lin, Z.H., Rao, Z.H., Tai, S.C., Chu, M.P., Li, L., Lin, J.F., 2017. Alteration of cholinergic anti-inflammatory pathway in rat with ischemic cardiomyopathy–modified electrophysiological function of heart. J. Am. Heart. Assoc. 6 (9), e006510.

Zhao, Y., Wang, J., Ballevre, O., Luo, H., Zhang, W., 2012. Antihypertensive effects and mechanisms of chlorogenic acids. Hypertens. Res. 35 (4), 370.